RAPID COMMUNICATIONS

PHYSICAL REVIEW E **73**, 065303(R) (2006)

Nonshielded multipolar vortices at high Reynolds number

L. A. Barba

Department of Mathematics, University of Bristol, Bristol BS8 1TW, United Kingdom

(Received 14 September 2005; revised manuscript received 6 March 2006; published 20 June 2006)

Vortex multipoles—consisting of a core of vorticity closely surrounded by several smaller vorticity concentrations of opposite sign—are obtained from the evolution of vorticity in two-dimensional simulations. Using a meshless vortex method, we obtained triangular and square vortices, surrounded by three and four satellites, respectively. These structures have only been observed before to emerge from zero-circulation initial conditions. We also observed a pentagon vortex. Here, we obtain compound vortices of nonzero total circulation, and suggest a gamut of multipolar asymptotic solutions to the Navier-Stokes equations.

DOI: 10.1103/PhysRevE.73.065303 PACS number(s): 47.32.C−, 47.20.−k

The most compelling phenomenon of two-dimensional (2D) turbulent flow is the self-organization of vorticity and the emergence of so-called coherent structures. Such a phenomenon has relevance for planetary flows, since the atmosphere and oceans are very close to two dimensional. Phenomena such as the longevity of eddies in the oceans, the creation of microclimates, and barriers to mixing come to mind [1]. Coherent vortices also appear in astrophysical problems, such as the Great Red Spot of Jupiter [2]. Moreover, the physics of relaxing 2D turbulence is analogous to the dynamics of pure-electron plasmas, allowing for significant experimental evidence of coherent vortex structures to be obtained from plasma experiments [3–5].

The study of coherent structures can be traced to the now classical numerical results of freely decaying turbulence [6] and the experimental realization of the Von Kármán vortex street in soap films [7]. In the first case, it was shown that vorticity concentrations arise spontaneously from a random field, and that they tend to assume axisymmetric shapes; the second gave a striking visualization of vortex dipoles. Thus arrived the two most common coherent structures: the monopole and the dipole. The tripole is a more rare object, seen to form from the collision of two dipoles [8] and appearing spontaneously in simulations of forced, homogeneous 2D turbulence [9]. The striking (and accidental) observation of a tripole in the laboratory was first reported in [10], and it was only later that a structure that could perhaps be a tripole was observed in the oceans for the first time [11]. Several investigations into this third coherent structure have followed, both experimental [12] and numerical [13,14]. Except for dipole collision, in all other occurrences the tripole emerged from the instability of axisymmetric shielded monopoles (i.e., a central vortex core surrounded by a ring of opposite sign vorticity, with zero total circulation). A surprising exception is the more recent numerical observation of a tripole obtained from the relaxation of a monopole to which a quadrupolar perturbation of moderate amplitude has been added [15]. In this case, it was expected that the perturbation would decay due to shear-enhanced diffusion [16,17], which occurs for small perturbations. But a large quadrupolar perturbation [Eq. (2), below, with $m=2$] introduces negative vorticity and markedly alters the evolution. Thus, it was suggested that a threshold amplitude of the quadrupole perturbation separates the basins of attraction of the monopole and tripole.

This Rapid Communication presents the result that a nonaxisymmetric component added to a Gaussian vortex can result in the reorganization of vorticity to form higher multipoles. Thus, the tripole found by Rossi *et al.* [15] is just one of a variety of vortex multipole solutions with nonzero total circulation. A six-pole nonaxisymmetric component [Eq. (2) with $m=3$], of sufficient amplitude, results in the reorganization of the flow into a *triangular vortex*. This rare object of 2D vortex flow, consisting of a core of vorticity with triangular shape surrounded by three satellites of opposite sign vorticity, has only been seen before emerging from shielded monopolar vortices; the profile of the initial shielded monopole in this case is steeper than those that generate tripoles [18,19]. We have found also that an eight-pole nonaxisymmetric component ($m=4$) is capable of generating a square vortex, in which four satellites surround a square-shaped core, and a ten-pole nonaxisymmetric component results in a pentagon vortex. These structures turn out to be unstable, and the vorticity re-organizes by satellite merging to form a tripole. As mentioned, when these exotic multipole vortices emerge from shielded monopoles, they have zero net circulation. In the present situation, they can emerge from a variety of initial conditions, and result in satellites of assorted strengths (relative to the core).

To be more precise, consider a flow with initial condition given by a Gaussian vortex with an added nonaxisymmetric component of m-fold symmetry; that is, $\omega=\omega_0+\omega'$ with

$$\omega_0(\mathbf{x}) = \frac{1}{4\pi}\exp\left(\frac{-|\mathbf{x}|^2}{4}\right), \tag{1}$$

$$\omega'(\mathbf{x}) = \frac{\delta}{4\pi}|\mathbf{x}|^2\exp\left(\frac{-|\mathbf{x}|^2}{4}\right)\cos m\theta, \tag{2}$$

where ω_0 stands for the base vortex, ω' for the nonaxisymmetric component, and $\theta=\arg(\mathbf{x})$. We will use the term "perturbation" for ω', even though it is of $O(1)$, for convenience. When $m=2$, it was found by Rossi *et al.* [15] that a tripole is obtained with $\delta=0.25$ at a Reynolds number $\mathrm{Re}=10^4$, where $\mathrm{Re}=\Gamma/\nu$ (total circulation divided by the viscosity). Figure 1 shows the vorticity evolution for this case. A vortex method has been used in this work, introduced by Barba *et al.* [20]; the numerical method is completely mesh-free and is characterized by very low numerical dissipation. For the simulation of Fig. 1, vortex particles were placed on a triangular

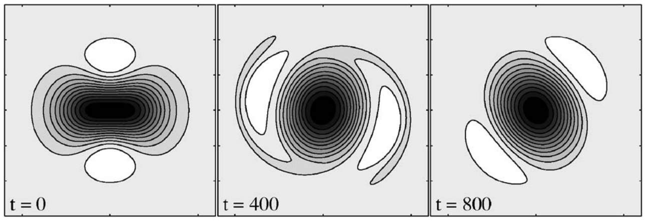

FIG. 1. Evolution of the tripolar vortex: 14 equally spaced contour levels of ω; Re$=10^4$, $\delta=0.25$.

lattice initially, with equivalent square interparticle spacing $h=0.15$; the initial core radius of particles was $\sigma=0.1875$, growing to a maximum radius (due to diffusion) of $\sigma=0.1901$ before spatial adaption. The number of particles was $N(t=0)=7138$ and $N(t=800)=9792$. The present results would be difficult to obtain with standard mesh-based methods, which suffer from numerical diffusion. Spectral methods are often preferred for vortex dynamics applications for this very reason, but then the use of hyperviscosity alters the physics, resulting, for example, in a different time scale for shear diffusion.

Consider now the striking result of using threefold symmetry in the perturbation. As shown in Fig. 2, the flow now reorganizes into a triangular vortex. Once revealed, this may seem as a natural result; it has not, however, been reported before, to our knowledge.

The triangular vortex has been previously discovered [18,19,21,22], but under very special conditions: emerging from the growth and saturation of instabilities in a strongly unstable monopolar vortex. The initial vorticity of the monopole depends on a steepness parameter α as follows: $\omega_\alpha=(0.5\alpha r^\alpha-1)e^{-r^\alpha}$. To obtain a triangle vortex, a steep initial profile is required with $\alpha\geqslant 5$. Figure 3 shows the evolution for $\alpha=7$, where the initialization with vortex particles was seeded with a perturbation of the form $r_{i,\mathrm{new}}=r_{i,\mathrm{old}}(1+\epsilon\sin k\theta)$ with $k=3$, $\epsilon=0.001$, and r_i the radial position of each vortex particle [29]. A similar result was obtained by Kloosterziel and Carnevale [22] using spectral methods. Experimental observations of the triangle vortex have been made both in rotating flow [19,21,23] and in stratified fluid [24].

Using the initial condition in Eqs. (1) and (2) with $m=3$, we obtain a range of triangle vortices, with the strength of the satellites becoming weaker as δ is decreased, until the vortex finally relaxes to axisymmetry. Thus, similarly to the tripole, it appears that a threshold perturbation amplitude separates the monopole and triangle vortices as asymptotic (quasisteady) states.

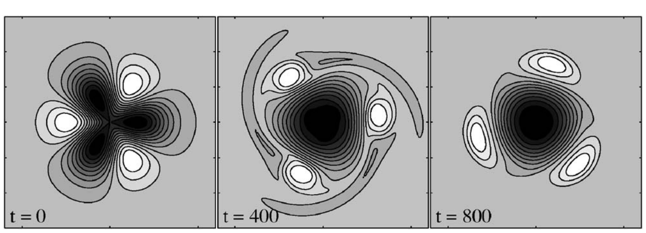

FIG. 2. Evolution of a triangular vortex: 14 equally spaced contour levels of ω; Re$=10^4$, $\delta=0.55$.

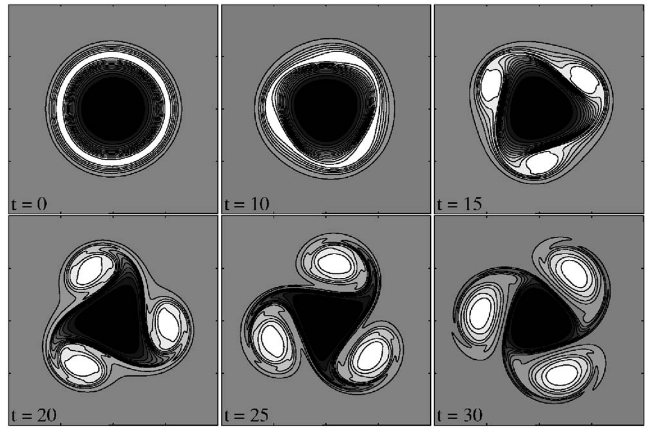

FIG. 3. Emergence of a triangular vortex from the saturated instability of a shielded monopole; 14 equally spaced contours of vorticity (black is negative, white is positive).

Note that the triangle vortex shown in Fig. 2 differs from that in Fig. 3 in the strength of the satellites, as well as the normalization. In the latter (shielded) case, the vorticity magnitude of the satellites and core is ≈ 1. In Fig. 2, the initial condition has $\omega_{\max}=0.1014$ and $\omega_{\min}=-0.0408$, whereas at $t=800$ $\omega_{\max}=0.0834$ and $\omega_{\min}=-0.0255$. Thus, the satellite peaks have a magnitude of only 30% compared to the vortex core. Also, the turnaround time $\tau=4\pi/\omega_{\max}$ for the shielded case is $\tau\approx 12$ and it is $\tau\approx 158$ for the vortex of Fig. 2 (which explains the different time scales in the figures).

The numerical parameters for the simulation in Fig. 2 are as follows: square-equivalent interparticle spacing $h=0.12$, initial vortex blob size $\sigma_0=0.15$, maximum size $\sigma_{\max}=0.1633$, number of particles $N_{t=0}=10\,660$, and $N_{t=800}=12\,586$. For the simulation in Fig. 3 $h=0.02$, $\sigma_0=0.025$, $\sigma_{\max}=0.0287$, $N_0=21\,216$, and $\nu=10^{-4}$.

For the flow of Fig. 2, it is most interesting to look at the evolution of the *perturbation* vorticity, obtained by subtracting the Lamb-Oseen vortex solution at each time slice; this is shown in Fig. 4. Note how the negative part of the perturbation drifts to the outside of the base Gaussian eddy, while the positive part coalesces toward the center and is subject to spiral wind-up. One could speculate that this is due to the "transverse drift" of vortices in a vorticity gradient [25], which is the same as vortex drifting in the β plane [26], but this needs further study. Subsequently, the positive perturba-

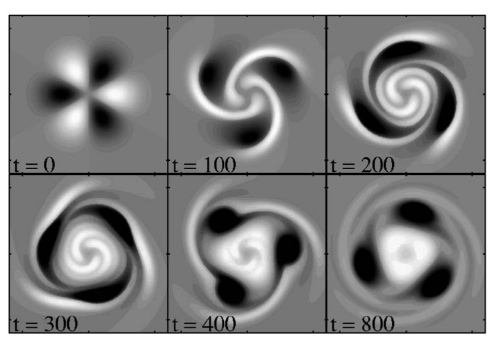

FIG. 4. Grayscale levels of perturbation vorticity; case Re$=10^4$, $\delta=0.55$ (cf. Fig. 2). Black is negative, white is positive.

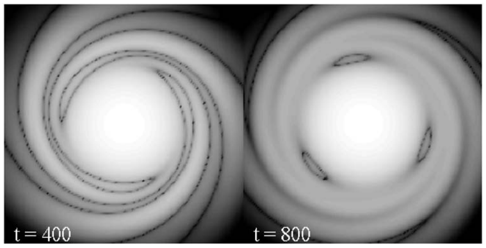

FIG. 5. Shadowed plot of $\log_{10}|\omega|$, emphasizing the boundary of the satellite vortices; case with $\delta=0.3$ and $\text{Re}=10^4$.

tion becomes homogenized in the center of the vortex, and the negative part forms well-defined satellite vortices. Weak positive filamentary debris surrounds the whole structure.

As mentioned, smaller values of δ result in weaker and weaker satellites, but the same structure. See for example Fig. 5, showing the logarithm of $|\omega|$ for the case $\delta=0.3$. When $\delta=0.25$, we observe the formation of a tiny closed zero contour of vorticity which immediately dissipates; even smaller values of δ result in complete axisymmetrization, with no intermediate triangle state.

A test of the stability of the triangle vortex was performed as follows. For a case developing moderate satellites, the flow was evolved until a time when the triangle vortex seems to be quasi steady. Then, the computational vortex particles were randomly perturbed; the resulting state is shown in the first frame of Fig. 6. Allowing this state to evolve freely, the perturbations smooth out, and the flow returns to a well-formed triangle vortex; see Fig. 6. This experiment indicates that the triangle vortex found here is a stable structure.

Naturally, the above results lead us to explore the effect of having an eight-pole perturbation ($m=4$). The nonlinear saturation of mode-4 instability generates a square vortex from very steep shielded monopoles [19,22]. This vortex was found to quickly break down, transitionally forming a tripole that further disintegrates into two dipoles. A square vortex has also been observed in stratified fluid experiments [30]. In the present situation, a square vortex can be formed with eight-pole perturbations from $\delta=0.6$ upward, with stronger satellites for larger δ. It was observed to undergo satellite merging and reorganize into a tripole. Moreover, a pentagon vortex can be formed from $\delta\approx 1.0$ upward; this vortex appears to be very unstable, and we observe merging of two pairs of satellites, to produce an asymmetric tripole. Figure 7 shows the evolution of the square and pentagon vortices and their transformation into tripoles.

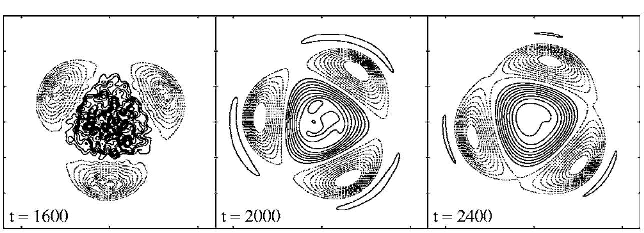

FIG. 6. Line contours of perturbation vorticity for a case with $\delta=0.7$ and $\text{Re}=10^4$, where the flow was perturbed at $t=1600$ by randomly moving all vortex particles.

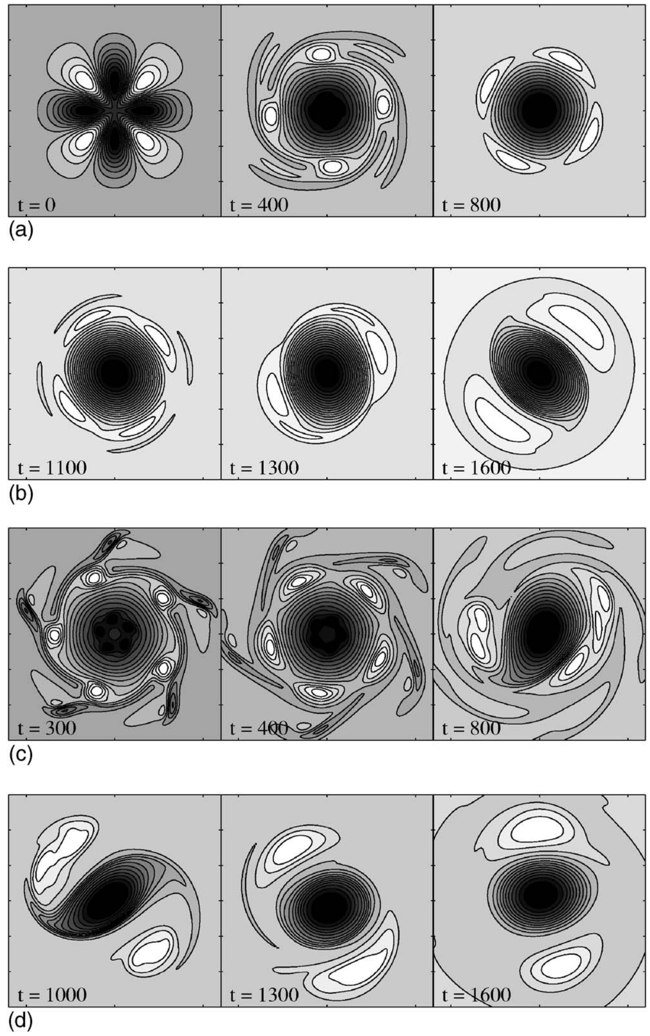

FIG. 7. Plots of ω for higher multipoles. Top two rows: square vortex; $\text{Re}=10^4$, $\delta=0.7$, $m=4$. Bottom two rows: pentagon vortex; $\text{Re}=10^4$, $\delta=1.2$, $m=5$.

In conclusion, we have shown that 2D vortex multipoles can be obtained from the re-organization of vorticity using various nonshielded initial conditions. The resulting multipoles do not have zero net circulation, and both the tripole and triangle vortex appear to be stable. Previous studies have focused on the growth and saturation of instabilities of shielded monopoles, and have indeed suggested that only the tripole and the triangular vortex are stable. We observe that the square vortex reorganizes by satellite merging into a tripole, whereas the pentagon vortex evolves into an asymmetric tripole. It is our belief that the mechanism operating in the emergence of multipoles from unstable shielded monopoles may be at play as well in the present situation of varying strength satellites. This mechanism is not well understood, and is worthy of further study. The results presented here will be valuable in this undertaking.

There are vortical structures in plasmas that are remarkably similar to the multipoles, exhibiting an asymmetry able to persist with very slow decay. For example, an elliptical core with two surrounding cat's eyes is shown in [3], whereas a triangular core with three cat's eyes appears in

[27]. These structures, called quasimodes, arise from initial conditions where vorticity is of only one sign—unlike the hydrodynamic multipoles. They are characterized by an angular frequency Ω_q and decay rate γ. The question arises of whether core quasimodes may be the cause of multipole vortex formation. We can present evidence that they are likely to be different objects. The $m=2$ quasimode frequency for a Gaussian vortex has been calculated to be $\Omega_q=0.226\omega_0(0)$ [28]. For the initial condition in this paper, $\omega_0(0)=1/4\pi$, giving $\Omega_q=0.018$. For the tripole in Fig. 1, after the initial rearrangement the angular velocity was found to oscillate around 0.01; this is quite different from Ω_q, and thus we conclude that the mechanism of multipole formation is unlikely to be caused by a quasimode.

ACKNOWLEDGMENTS

Computing time from Bristol Laboratory for Advanced Computation in the Mathematical Sciences (http://lacms.maths.bris.ac.uk/) is acknowledged. Thanks to G. J. F. van Heijst and P. Orlandi for comments on the draft.

[1] E. J. Hopfinger and G. J. F. van Heijst, Annu. Rev. Fluid Mech. **25**, 241 (1993).
[2] P. S. Marcus, Annu. Rev. Astron. Astrophys. **31**, 523 (1993).
[3] C. F. Driscoll and K. S. Fine, Phys. Fluids B **2**, 1359 (1990).
[4] X. P. Huang and C. F. Driscoll, Phys. Rev. Lett. **72**, 2187 (1994).
[5] C. F. Driscoll, D. Z. Jin, D. A. Schecter, and D. H. E. Dubin, Physica C **369**, 21 (2002).
[6] J. C. McWilliams, J. Fluid Mech. **146**, 21 (1984).
[7] Y. Couder and C. Basdevant, J. Fluid Mech. **173**, 225 (1986).
[8] V. D. Larichev and G. M. Reznik, Okeanologiya **23**, 545 (1983).
[9] B. Legras, P. Santangelo, and R. Benzi, Europhys. Lett. **5**, 37 (1988).
[10] G. J. F. van Heijst and R. C. Kloosterziel, Nature (London) **338**, 569 (1989).
[11] R. D. Pingree and B. Le Cann, Deep-Sea Res., Part A **39**, 1147 (1992).
[12] G. J. F. van Heijst, R. C. Kloosterziel, and C. W. M. Williams, J. Fluid Mech. **225**, 301 (1991).
[13] X. J. Carton, G. R. Flierl, and L. M. Polvani, Europhys. Lett. **9**, 339 (1989).
[14] L. M. Polvani and X. J. Carton, Geophys. Astrophys. Fluid Dyn. **51**, 87 (1990).
[15] L. F. Rossi, J. F. Lingevitch, and A. J. Bernoff, Phys. Fluids **9**, 2329 (1997).
[16] T. S. Lundgren, Phys. Fluids **25**, 2193 (1982).
[17] A. J. Bernoff and J. F. Lingevitch, Phys. Fluids **6**, 3717 (1994).
[18] P. Orlandi and G. J. F. van Heijst, Fluid Dyn. Res. **9**, 179 (1992).
[19] G. F. Carnevale and R. C. Kloosterziel, J. Fluid Mech. **259**, 305 (1994).
[20] L. A. Barba, A. Leonard, and C. B. Allen, Int. J. Numer. Methods Fluids **47**, 387 (2005).
[21] M. Beckers and G. J. F. van Heijst, Fluid Dyn. Res. **22**, 265 (1998).
[22] R. C. Kloosterziel and G. F. Carnevale, J. Fluid Mech. **388**, 217 (1999).
[23] R. C. Kloosterziel and G. J. F. van Heijst, J. Fluid Mech. **223**, 1 (1991).
[24] J. B. Flór and G. J. F. van Heijst, J. Fluid Mech. **311**, 257 (1996).
[25] D. A. Schecter and D. H. E. Dubin, Phys. Rev. Lett. **83**, 2191 (1999).
[26] G. F. Carnevale, R. C. Kloosterziel, and G. J. F. van Heijst, J. Fluid Mech. **233**, 119 (1991).
[27] T. B. Mitchell and C. F. Driscoll, Phys. Rev. Lett. **73**, 2196 (1994).
[28] D. A. Schecter, D. H. E. Dubin, A. C. Cass, C. F. Driscoll, I. M. Lansky, and T. M. O'Neill, Phys. Fluids **12**, 2397 (2000).
[29] We initialized with a data file of particle information provided by G. Daenick (private communication).
[30] M. Beckers and G. J. F. van Heijst (private communication), http://www.fluid.tue. nl/WDY/vort/instab/strat/strat.html